Ain Shams University Faculty of Science Chemistry Department



Study on utility of nano-semiconductors in solar cells

A Thesis

Submitted for the Degree of Master of Science
As Partial Fulfillment for Requirements of Master of Science
"Chemistry Department"

 $\mathbf{B}\mathbf{y}$

Amr Mohamed Ahmed Elattar

B.Sc. in Applied Chemistry, Faculty of Science
Ain Shams University
2011

Under Supervision of

Dr. Mostafa Mohamed Hassan Khalil

Professor of inorganic Chemistry, Faculty of Science, Ain Shams University

Dr. Fawzy Abdel Hameed Mahmoud

Associate Professor of Physics
National Research Center

Ain Shams University Faculty of Science Chemistry Department



Approval Sheet

Study on utility of nano-semiconductors in solar cells

$\mathbf{B}\mathbf{y}$

Amr Mohamed Ahmed Elattar

B.Sc. in applied chemistry, Faculty of Science
Ain Shams University
2011

This thesis for Master degree has been approved by:

Dr. Mostafa Mohamed Hassan Khalil

Professor of inorganic Chemistry, Faculty of Science, Ain Shams University

Dr. Fawzy Abdel Hameed Mahmoud

Associate Professor of Physics, National Research Center

Head of Chemistry Department Prof. Dr. Ibrahim Hussainy Ali Badr

Ain Shams University Faculty of Science Chemistry Department



Student Name: Amr Mohamed Ahmed Elattar

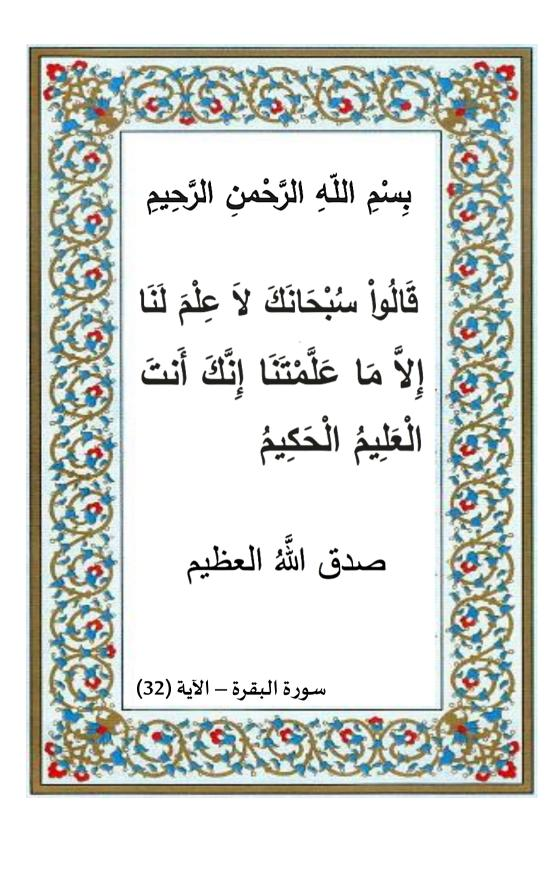
Scientific Degree: M.Sc.

Faculty Name: Faculty of Science – Ain Shams University

Graduation Year: 2011

Granting Year:

Head of Chemistry Department Prof. Dr. Ibrahim Hussainy Ali Badr



Acknowledgement

First I do thank Allah the most merciful for his indefinite blessings

I am indebted to **Prof. Dr. Mostafa M. H. Khalil**, Professor of Inorganic and Analytical
Chemistry, Faculty of Science, Ain Shams
University, for suggesting the theme of this study,
for the help and guidance he has given during his
supervision of this work and without which
fulfillment of this work would be impossible, for
helping and revising the whole manuscript.

I would like to express my deepest appreciation to Dr. Fawzy A. Mahmoud, Assistant Professor of Physics Department, National Research Center, for offering me the opportunity to carry out this interesting research work under her kind supervision and guidance and for his helping me for writing the thesis.

Contents

List of Tables and Schemes
List of Figuresii
Aim of the workiii
Summaryiv
Chapter 1: Introduction
1.1 Introduction of nanotechnology2
1.2 History of nanomaterials
1.3 Semiconductor Nanocrystals6
1.3.1 Quantum Confinement Effect6
1.3.2 Quantum Dots Classification9
1.3.3 Characteristics of QDs11
1.3.3.1 Size-dependent effect
1.3.3.2 Multiple Exciton Generation (MEG)13
1.3.4 Quantum Dots Applications
1.3.4.1 Electroluminescence Device Fabrication16
1.3.4.2 Downconversion of Blue or Ultraviolet Light17
1.3.4.3 Bioimaging Applications
1.3.4.4 Other Optoelectronic Devices
1.3.4.5 Quantum Dots in Solar Cell Device Fabrication20
1.3.4.5.1 Quantum Dot Dispersed Solar Cell23
1.3.4.5.2 Quantum Dot Sensitized Solar Cell (QDSSCs)23
1.3.4.5.2.1 Basic Principle of n-type QDSSCs24
1.3.4.5.2.2 P-type QDSSCs

1.3.5 Quantum Dots Synthesis	29
1.3.5.1 Top-Down Synthesis Processes	
1.3.5.2.1 Wet-Chemical Methods	
1.3.5.2.1.2 Microemulsion Process	32
1.3.5.2.1.3 Hot-Solution Decomposition Process	33
1.3.5.2.1.4 Sonic waves or microwaves	34
1.3.5.2.1.5 Hydrothermal synthesis	35
1.3.5.2.2 Vapor-Phase Methods	36
1.3.5.2.2.1 Molecular beam epitaxy (MBE)	36
1.3.5.2.2.2 Physical vapor deposition (PVD)	37
1.3.5.2.2.3 Chemical vapor deposition (CVD)	37
1.3.6 Methods of assembly of quantum dots on wide- bandgap	
semiconductor (TiO ₂) layer	38
1.3.6.1 In-situ preparation	38
1.3.6.1.1 Chemical bath deposition (CBD)	38
1.3.6.1.2 Successive ionic-layer adsorption and reaction (SILAR)	38
1.3.6.2 Ex-situ preparation	40
1.3.6.2.1 Monodisperse QDs with Molecular Linkers	40
1.3.6.2.2 Direct Adsorption (DA)	42
1.3.7Characterization	43
1.3.7.1 Quantum Dots characterization	43
1.3.7.1.1 X-ray diffraction (XRD)	43
1.3.7.1.2 Transmission electron microscope (TEM)	43
1.3.7.1.3 Electron diffraction spectroscopy (EDS)	43

1.3.7.1.4 Fourier transfer infra-red (FTIR)44
1.3.7.1.5 Raman Spectra
1.3.7.1.6 X-ray photoelectron spectroscopy (XPS)44
1.3.7.1.7 Ultraviolet-visible spectrophotometer (UV-Vis)
1.3.7.2 Solar cell characterization45
1.3.8 Literature review47
Chapter 2: Experimental work
2.1. Chemicals53
2.2. Methodology53
2.2.1. Preparation of different types of Quantum Dots54
2.2.1.1 CdSe/CdS core/shell QDs54
2.2.1.1.1 Wet chemical 3-neck round bottom flask method54
2.2.1.1.1 In-situ hydrothermal method56
2.2.1.2 CdTe/ CdS core/shell QDs56
2.2.1.3 CdZnSe/CdS and CdZnSe/ZnS core/shell QDs58
2.2.1.4 CdZnSe/CdS and CdZnSe/ZnS core/shell QDs59
2.2.1.5 CdSeTe/CdS core/shell QDs61
2.2.1.6 CdZnSeTe/CdS and CdZnSeTe/ZnS core/shell QDs62
2.2.1.7 CuZnS QDs64
2.2.2 Preparation of TiO ₂ thin films66
2.2.3 Preparation of TiO ₂ / QDs thin films67

2.2.4 ZnS Passive layer formation69
2.2.5 Electrolyte preparation69
2.2.6 Counter Electrode preparation69
2.2.7 QDSSC Fabrication70
2.3 Characterization70
Chapter 3: Results and Discussion
3.1 Quantum Dots Characterization72
3.1.1 CdSe/CdS core/shell QDs72
3.1.1.1 3 Wet chemical method72
3.1.1.2 In-situ hydrothermal method82
3.1.2 CdTe/ CdS core/shell QDs88
3.1.3 CdZnSe/CdS and CdZnSe/ZnS core/shell QDs94
3.1.4 CdZnSe/CdS and CdZnSe/ZnS core/shell QDs100
3.1.5 CdSeTe/CdS core/shell QDs106
3.1.6 CdZnSeTe/CdS and CdZnSeTe/ZnS core/shell QDs112
3.1.7 CuZnS QDs117
3.2 QDSSCs Characterization123
3.2.1 CdSe/CdS core/shell QDSSCs
Anabia Summany

List of tables and schemes

Scheme 2.1	preparation reaction mechanism of CdSe/CdS core/shell QDs.
Scheme 2.2	preparation reaction mechanism of CdTe/CdS core/shell QDs.
Scheme 2.3	preparation reaction mechanism of CdZnSe/CdS and CdZnSe/ZnS core/shell QDs.
Scheme 2.4	preparation reaction mechanism of CdZnTe/CdS and CdZnTe/ZnS core/shell QDs.
Scheme 2.5	preparation reaction mechanism of CdSeTe/CdS core/shell QDs.
Scheme 2.6	preparation reaction mechanism of CdZnSeTe/CdS and CdZnSeTe/ZnS core/shell QDs.
Table1.1	Classification of QDs.

List of figures

Figure (1.1)	Famous 4th century Roman cup.
Figure (1.2)	The density of states, DOS, of bulk materials, quantum wells, quantum rods and quantum dots.
Figure (1.3)	Absorption and Photoluminescence (PL) spectra of colloidal CdSe.
Figure (1.4)	Relation between the size and bandgap of CdSe QDs.
Figure (1.5)	(A) Conventional semiconductor QDs and (B) multiple excitons, MEG, are generated under the effect of a single phonon.
Figure(1.6)	Classification of quantum dots solar cells: A) P-I-N solar cell, B) QDs sensitized solar cell and C) QDs dispersed solar cell (Nozik, 2002).
Figure (1.7)	(n-type) quantum dots sensitized solar cells
Figure (1.8)	Schematic of an energy diagram of a QDSSC stack under flat band conditions. Key processes leading to the generation of photocurrent are shown in (a)–(e).
Figure (1.9)	Energy level diagram for (a) n-type and (b) p-type QDSCs.
Figure (1.10)	Schematics of a SILAR cycle: (1) adsorption of the metal precursor, (2,4) wash and (3) surface reaction.
Figure (1.11)	Connection between TiO ₂ and QDs with a bifunctional molecule as linker.
Figure (1.12)	Typical J–V (Black curve) and P–V (Red curve) relations of a QDSSC.
Figure (2.1)	CZS QDs representation.

Figure (2.2) FTO and FTO/ TiO₂ from our lab. Figure (2.3) CdSe QDs at different temperatures. Figure (2.4) Different quantum dots assembly on mixed TiO₂ paste at 170°C. Figure (2.5) Different quantum dots assembly on solaronix TiO₂ paste at 170°C. Figure (3.1) Electron diffraction spectroscopy (EDS) of CdSe/CdS core/shell QDs (S1). Figure (3.2) HRTEM images of CdSe QDs of the studied samples with particle sizes 1.62.2 nm (image 1), 1.68-2.29 nm (image 2), 1.8-2.4 nm (image 3), 2.9-3.3 nm (image 4) and 4.8-5.4 nm (image 5) as a function of TGA in mL. Figure (3.3) UV-Vis spectra of CdSe/CdS core/shell QDs. Figure (3.4) The color of CdSe/CdS core/shell QDs. Figure (3.5) Relation between of CdSe/CdS core/shell QDs. Figure (3.6) Bandgap of CdSe/CdS core/shell QDs. Figure (3.7) Relation between CdSe/CdS core/shell QDs bandgap and TGA capping agent amount. Figure (3.8) Photoluminescence (PL) spectra of CdSe/CdS core/shell QDs. Figure (3.9) Electron diffraction spectroscopy (EDS) of CdSe/CdS core/shell QDs prepared via hydrothermal method. Figure (3.10) FT-IR spectrum of CdSe/CdS core/shell QDs prepared via hydrothermal method. Figure (3.11) XRD θ-2θ pattern of CdSe/CdS core/shell nanocrystals.	Figure (2.3) CdSe QDs at different temperatures. Figure (2.4) Different quantum dots assembly on mixed TiO₂ paste at 170°C. Figure (2.5) Different quantum dots assembly on solaronix TiO₂ paste at 170°C. Figure (3.1) Electron diffraction spectroscopy (EDS) of CdSe/CdS core/shell QDs (S1). Figure (3.2) HRTEM images of CdSe QDs of the studied samples with particle sizes 1.62.2 nm (image 1), 1.68-2.29 nm (image 2), 1.8-2.4 nm (image 3), 2.9-3.3 nm (image 4) and 4.8-5.4 nm (image 5) as a function of TGA in mL. Figure (3.3) UV-Vis spectra of CdSe/CdS core/shell QDs. Figure (3.4) The color of CdSe/CdS core/shell QDs. Figure (3.5) Relation between of CdSe/CdS core/shell QDs. Figure (3.6) Bandgap of CdSe/CdS core/shell QDs. Figure (3.7) Relation between CdSe/CdS core/shell QDs bandgap and TGA capping agent amount. Figure (3.8) Photoluminescence (PL) spectra of CdSe/CdS core/shell QDs. Figure (3.9) Electron diffraction spectroscopy (EDS) of CdSe/CdS core/shell QDs prepared via hydrothermal method. Figure (3.10) FT-IR spectrum of CdSe/CdS core/shell QDs prepared via hydrothermal method. Figure (3.11) XRD θ-2θ pattern of CdSe/CdS core/shell nanocrystals.		
Figure (2.4) Different quantum dots assembly on mixed TiO2 paste at 170°C. Figure (2.5) Different quantum dots assembly on solaronix TiO2 paste at 170°C. Figure (3.1) Electron diffraction spectroscopy (EDS) of CdSe/CdS core/shell QDs (S1). Figure (3.2) HRTEM images of CdSe QDs of the studied samples with particle sizes 1.62.2 nm (image 1), 1.68-2.29 nm (image 2), 1.8-2.4 nm (image 3), 2.9-3.3 nm (image 4) and 4.8-5.4 nm (image 5) as a function of TGA in mL. Figure (3.3) UV-Vis spectra of CdSe/CdS core/shell QDs. Figure (3.4) The color of CdSe/CdS core/shell QDs. Figure (3.5) Relation between of CdSe/CdS core/shell QDs. Figure (3.6) Bandgap of CdSe/CdS core/shell QDs. Figure (3.7) Relation between CdSe/CdS core/shell QDs bandgap and TGA capping agent amount. Figure (3.8) Photoluminescence (PL) spectra of CdSe/CdS core/shell QDs. Figure (3.9) Electron diffraction spectroscopy (EDS) of CdSe/CdS core/shell QDs prepared via hydrothermal method. Figure (3.10) FT-IR spectrum of CdSe/CdS core/shell QDs prepared via hydrothermal method.	Figure (2.4) Different quantum dots assembly on mixed TiO ₂ paste at 170°C. Figure (2.5) Different quantum dots assembly on solaronix TiO ₂ paste at 170°C. Figure (3.1) Electron diffraction spectroscopy (EDS) of CdSe/CdS core/shell QDs (S1). Figure (3.2) HRTEM images of CdSe QDs of the studied samples with particle sizes 1.62.2 nm (image 1), 1.68-2.29 nm (image 2), 1.8-2.4 nm (image 3), 2.9-3.3 nm (image 4) and 4.8-5.4 nm (image 5) as a function of TGA in mL. Figure (3.3) UV-Vis spectra of CdSe/CdS core/shell QDs. Figure (3.4) The color of CdSe/CdS core/shell QDs. Figure (3.5) Relation between of CdSe/CdS core/shell QDs size and TGA capping agent amount. Figure (3.6) Bandgap of CdSe/CdS core/shell QDs. Figure (3.7) Relation between CdSe/CdS core/shell QDs bandgap and TGA capping agent amount. Figure (3.8) Photoluminescence (PL) spectra of CdSe/CdS core/shell QDs. Figure (3.9) Electron diffraction spectroscopy (EDS) of CdSe/CdS core/shell QDs prepared via hydrothermal method. Figure (3.10) FT-IR spectrum of CdSe/CdS core/shell QDs prepared via hydrothermal method. Figure (3.11) XRD θ-2θ pattern of CdSe/CdS core/shell nanocrystals.	Figure (2.2)	FTO and FTO/ TiO ₂ from our lab.
Figure (2.5) Different quantum dots assembly on solaronix TiO₂ paste at 170°C. Figure (3.1) Electron diffraction spectroscopy (EDS) of CdSe/CdS core/shell QDs (S1). Figure (3.2) HRTEM images of CdSe QDs of the studied samples with particle sizes 1.62.2 nm (image 1), 1.68-2.29 nm (image 2), 1.8-2.4 nm (image 3), 2.9-3.3 nm (image 4) and 4.8-5.4 nm (image 5) as a function of TGA in mL. Figure (3.3) UV-Vis spectra of CdSe/CdS core/shell QDs. Figure (3.4) The color of CdSe/CdS core/shell QDs. Figure (3.5) Relation between of CdSe/CdS core/shell QDs size and TGA capping agent amount. Figure (3.6) Bandgap of CdSe/CdS core/shell QDs. Figure (3.7) Relation between CdSe/CdS core/shell QDs bandgap and TGA capping agent amount. Figure (3.8) Photoluminescence (PL) spectra of CdSe/CdS core/shell QDs. Figure (3.9) Electron diffraction spectroscopy (EDS) of CdSe/CdS core/shell QDs prepared via hydrothermal method. Figure (3.10) FT-IR spectrum of CdSe/CdS core/shell QDs prepared via hydrothermal method.	Figure (2.5) Different quantum dots assembly on solaronix TiO ₂ paste at 170°C. Figure (3.1) Electron diffraction spectroscopy (EDS) of CdSe/CdS core/shell QDs (S1). Figure (3.2) HRTEM images of CdSe QDs of the studied samples with particle sizes 1.62.2 nm (image 1), 1.68-2.29 nm (image 2), 1.8-2.4 nm (image 3), 2.9-3.3 nm (image 4) and 4.8-5.4 nm (image 5) as a function of TGA in mL. Figure (3.3) UV-Vis spectra of CdSe/CdS core/shell QDs. Figure (3.4) The color of CdSe/CdS core/shell QDs. Figure (3.5) Relation between of CdSe/CdS core/shell QDs size and TGA capping agent amount. Figure (3.6) Bandgap of CdSe/CdS core/shell QDs. Figure (3.7) Relation between CdSe/CdS core/shell QDs bandgap and TGA capping agent amount. Figure (3.8) Photoluminescence (PL) spectra of CdSe/CdS core/shell QDs. Figure (3.9) Electron diffraction spectroscopy (EDS) of CdSe/CdS core/shell QDs prepared via hydrothermal method. Figure (3.10) FT-IR spectrum of CdSe/CdS core/shell QDs prepared via hydrothermal method. Figure (3.11) XRD θ-2θ pattern of CdSe/CdS core/shell nanocrystals.	Figure (2.3)	CdSe QDs at different temperatures.
Figure (3.1) Electron diffraction spectroscopy (EDS) of CdSe/CdS core/shell QDs (S1). Figure (3.2) HRTEM images of CdSe QDs of the studied samples with particle sizes 1.62.2 nm (image 1), 1.68-2.29 nm (image 2), 1.8-2.4 nm (image 3), 2.9-3.3 nm (image 4) and 4.8-5.4 nm (image 5) as a function of TGA in mL. Figure (3.3) UV-Vis spectra of CdSe/CdS core/shell QDs. Figure (3.4) The color of CdSe/CdS core/shell QDs. Figure (3.5) Relation between of CdSe/CdS core/shell QDs size and TGA capping agent amount. Figure (3.6) Bandgap of CdSe/CdS core/shell QDs. Figure (3.7) Relation between CdSe/CdS core/shell QDs bandgap and TGA capping agent amount. Figure (3.8) Photoluminescence (PL) spectra of CdSe/CdS core/shell QDs. Figure (3.9) Electron diffraction spectroscopy (EDS) of CdSe/CdS core/shell QDs prepared via hydrothermal method. Figure (3.10) FT-IR spectrum of CdSe/CdS core/shell QDs prepared via hydrothermal method.	Figure (3.1) Electron diffraction spectroscopy (EDS) of CdSe/CdS core/shell QDs (S1). Figure (3.2) HRTEM images of CdSe QDs of the studied samples with particle sizes 1.62.2 nm (image 1), 1.68-2.29 nm (image 2), 1.8-2.4 nm (image 3), 2.9-3.3 nm (image 4) and 4.8-5.4 nm (image 5) as a function of TGA in mL. Figure (3.3) UV-Vis spectra of CdSe/CdS core/shell QDs. Figure (3.4) The color of CdSe/CdS core/shell QDs. Figure (3.5) Relation between of CdSe/CdS core/shell QDs size and TGA capping agent amount. Figure (3.6) Bandgap of CdSe/CdS core/shell QDs. Figure (3.7) Relation between CdSe/CdS core/shell QDs bandgap and TGA capping agent amount. Figure (3.8) Photoluminescence (PL) spectra of CdSe/CdS core/shell QDs. Figure (3.9) Electron diffraction spectroscopy (EDS) of CdSe/CdS core/shell QDs prepared via hydrothermal method. Figure (3.10) FT-IR spectrum of CdSe/CdS core/shell QDs prepared via hydrothermal method. Figure (3.11) XRD θ-2θ pattern of CdSe/CdS core/shell nanocrystals.	Figure (2.4)	Different quantum dots assembly on mixed TiO ₂ paste at 170°C.
Figure (3.2) HRTEM images of CdSe QDs of the studied samples with particle sizes 1.62.2 nm (image 1), 1.68-2.29 nm (image 2), 1.8-2.4 nm (image 3), 2.9-3.3 nm (image 4) and 4.8-5.4 nm (image 5) as a function of TGA in mL. Figure (3.3) UV-Vis spectra of CdSe/CdS core/shell QDs. Figure (3.4) The color of CdSe/CdS core/shell QDs. Figure (3.5) Relation between of CdSe/CdS core/shell QDs size and TGA capping agent amount. Figure (3.6) Bandgap of CdSe/CdS core/shell QDs. Figure (3.7) Relation between CdSe/CdS core/shell QDs bandgap and TGA capping agent amount. Figure (3.8) Photoluminescence (PL) spectra of CdSe/CdS core/shell QDs. Figure (3.9) Electron diffraction spectroscopy (EDS) of CdSe/CdS core/shell QDs prepared via hydrothermal method. Figure (3.10) FT-IR spectrum of CdSe/CdS core/shell QDs prepared via hydrothermal method.	Figure (3.2) HRTEM images of CdSe QDs of the studied samples with particle sizes 1.62.2 nm (image 1), 1.68-2.29 nm (image 2), 1.8-2.4 nm (image 3), 2.9-3.3 nm (image 4) and 4.8-5.4 nm (image 5) as a function of TGA in mL. Figure (3.3) UV-Vis spectra of CdSe/CdS core/shell QDs. Figure (3.4) The color of CdSe/CdS core/shell QDs. Figure (3.5) Relation between of CdSe/CdS core/shell QDs size and TGA capping agent amount. Figure (3.6) Bandgap of CdSe/CdS core/shell QDs. Figure (3.7) Relation between CdSe/CdS core/shell QDs bandgap and TGA capping agent amount. Figure (3.8) Photoluminescence (PL) spectra of CdSe/CdS core/shell QDs. Figure (3.9) Electron diffraction spectroscopy (EDS) of CdSe/CdS core/shell QDs prepared via hydrothermal method. Figure (3.10) FT-IR spectrum of CdSe/CdS core/shell QDs prepared via hydrothermal method. Figure (3.11) XRD 0-20 pattern of CdSe/CdS core/shell nanocrystals.	Figure (2.5)	Different quantum dots assembly on solaronix TiO ₂ paste at 170°C.
nm (image 1), 1.68-2.29 nm (image 2), 1.8-2.4 nm (image 3), 2.9-3.3 nm (image 4) and 4.8-5.4 nm (image 5) as a function of TGA in mL. Figure (3.3) UV-Vis spectra of CdSe/CdS core/shell QDs. Figure (3.4) The color of CdSe/CdS core/shell QDs. Figure (3.5) Relation between of CdSe/CdS core/shell QDs size and TGA capping agent amount. Figure (3.6) Bandgap of CdSe/CdS core/shell QDs. Figure (3.7) Relation between CdSe/CdS core/shell QDs bandgap and TGA capping agent amount. Figure (3.8) Photoluminescence (PL) spectra of CdSe/CdS core/shell QDs. Figure (3.9) Electron diffraction spectroscopy (EDS) of CdSe/CdS core/shell QDs prepared via hydrothermal method. Figure (3.10) FT-IR spectrum of CdSe/CdS core/shell QDs prepared via hydrothermal method.	nm (image 1), 1.68-2.29 nm (image 2), 1.8-2.4 nm (image 3), 2.9-3.3 nm (image 4) and 4.8-5.4 nm (image 5) as a function of TGA in mL. Figure (3.3) UV-Vis spectra of CdSe/CdS core/shell QDs. Figure (3.4) The color of CdSe/CdS core/shell QDs. Figure (3.5) Relation between of CdSe/CdS core/shell QDs size and TGA capping agent amount. Figure (3.6) Bandgap of CdSe/CdS core/shell QDs. Figure (3.7) Relation between CdSe/CdS core/shell QDs bandgap and TGA capping agent amount. Figure (3.8) Photoluminescence (PL) spectra of CdSe/CdS core/shell QDs. Figure (3.9) Electron diffraction spectroscopy (EDS) of CdSe/CdS core/shell QDs prepared via hydrothermal method. Figure (3.10) FT-IR spectrum of CdSe/CdS core/shell QDs prepared via hydrothermal method. Figure (3.11) XRD θ-2θ pattern of CdSe/CdS core/shell nanocrystals.	Figure (3.1)	Electron diffraction spectroscopy (EDS) of CdSe/CdS core/shell QDs (S1).
nm (image 1), 1.68-2.29 nm (image 2), 1.8-2.4 nm (image 3), 2.9-3.3 nm (image 4) and 4.8-5.4 nm (image 5) as a function of TGA in mL. Figure (3.3) UV-Vis spectra of CdSe/CdS core/shell QDs. Figure (3.4) The color of CdSe/CdS core/shell QDs. Figure (3.5) Relation between of CdSe/CdS core/shell QDs size and TGA capping agent amount. Figure (3.6) Bandgap of CdSe/CdS core/shell QDs. Figure (3.7) Relation between CdSe/CdS core/shell QDs bandgap and TGA capping agent amount. Figure (3.8) Photoluminescence (PL) spectra of CdSe/CdS core/shell QDs. Figure (3.9) Electron diffraction spectroscopy (EDS) of CdSe/CdS core/shell QDs prepared via hydrothermal method. Figure (3.10) FT-IR spectrum of CdSe/CdS core/shell QDs prepared via hydrothermal method.	nm (image 1), 1.68-2.29 nm (image 2), 1.8-2.4 nm (image 3), 2.9-3.3 nm (image 4) and 4.8-5.4 nm (image 5) as a function of TGA in mL. Figure (3.3) UV-Vis spectra of CdSe/CdS core/shell QDs. Figure (3.4) The color of CdSe/CdS core/shell QDs. Figure (3.5) Relation between of CdSe/CdS core/shell QDs size and TGA capping agent amount. Figure (3.6) Bandgap of CdSe/CdS core/shell QDs. Figure (3.7) Relation between CdSe/CdS core/shell QDs bandgap and TGA capping agent amount. Figure (3.8) Photoluminescence (PL) spectra of CdSe/CdS core/shell QDs. Figure (3.9) Electron diffraction spectroscopy (EDS) of CdSe/CdS core/shell QDs prepared via hydrothermal method. Figure (3.10) FT-IR spectrum of CdSe/CdS core/shell QDs prepared via hydrothermal method. Figure (3.11) XRD θ-2θ pattern of CdSe/CdS core/shell nanocrystals.	Figure (3.2)	HRTEM images of CdSe ODs of the studied samples with particle sizes 1.62.2
4) and 4.8-5.4 nm (image 5) as a function of TGA in mL. Figure (3.3) UV-Vis spectra of CdSe/CdS core/shell QDs. Figure (3.4) The color of CdSe/CdS core/shell QDs. Figure (3.5) Relation between of CdSe/CdS core/shell QDs size and TGA capping agent amount. Figure (3.6) Bandgap of CdSe/CdS core/shell QDs. Figure (3.7) Relation between CdSe/CdS core/shell QDs bandgap and TGA capping agent amount. Figure (3.8) Photoluminescence (PL) spectra of CdSe/CdS core/shell QDs. Figure (3.9) Electron diffraction spectroscopy (EDS) of CdSe/CdS core/shell QDs prepared via hydrothermal method. Figure (3.10) FT-IR spectrum of CdSe/CdS core/shell QDs prepared via hydrothermal method.	 4) and 4.8-5.4 nm (image 5) as a function of TGA in mL. Figure (3.3) UV-Vis spectra of CdSe/CdS core/shell QDs. Figure (3.4) The color of CdSe/CdS core/shell QDs. Figure (3.5) Relation between of CdSe/CdS core/shell QDs size and TGA capping agent amount. Figure (3.6) Bandgap of CdSe/CdS core/shell QDs. Figure (3.7) Relation between CdSe/CdS core/shell QDs bandgap and TGA capping agent amount. Figure (3.8) Photoluminescence (PL) spectra of CdSe/CdS core/shell QDs. Figure (3.9) Electron diffraction spectroscopy (EDS) of CdSe/CdS core/shell QDs prepared via hydrothermal method. Figure (3.10) FT-IR spectrum of CdSe/CdS core/shell QDs prepared via hydrothermal method. Figure (3.11) XRD θ-2θ pattern of CdSe/CdS core/shell nanocrystals. 	1.80.0 (0.2)	
Figure (3.4) The color of CdSe/CdS core/shell QDs. Figure (3.5) Relation between of CdSe/CdS core/shell QDs size and TGA capping agent amount. Figure (3.6) Bandgap of CdSe/CdS core/shell QDs. Figure (3.7) Relation between CdSe/CdS core/shell QDs. Figure (3.8) Photoluminescence (PL) spectra of CdSe/CdS core/shell QDs. Figure (3.9) Electron diffraction spectroscopy (EDS) of CdSe/CdS core/shell QDs prepared via hydrothermal method. Figure (3.10) FT-IR spectrum of CdSe/CdS core/shell QDs prepared via hydrothermal method.	Figure (3.3) UV-Vis spectra of CdSe/CdS core/shell QDs. Figure (3.4) The color of CdSe/CdS core/shell QDs. Figure (3.5) Relation between of CdSe/CdS core/shell QDs size and TGA capping agent amount. Figure (3.6) Bandgap of CdSe/CdS core/shell QDs. Figure (3.7) Relation between CdSe/CdS core/shell QDs bandgap and TGA capping agent amount. Figure (3.8) Photoluminescence (PL) spectra of CdSe/CdS core/shell QDs. Figure (3.9) Electron diffraction spectroscopy (EDS) of CdSe/CdS core/shell QDs prepared via hydrothermal method. Figure (3.10) FT-IR spectrum of CdSe/CdS core/shell QDs prepared via hydrothermal method. Figure (3.11) XRD θ-2θ pattern of CdSe/CdS core/shell nanocrystals.		
Figure (3.4) The color of CdSe/CdS core/shell QDs. Figure (3.5) Relation between of CdSe/CdS core/shell QDs size and TGA capping agent amount. Figure (3.6) Bandgap of CdSe/CdS core/shell QDs. Figure (3.7) Relation between CdSe/CdS core/shell QDs bandgap and TGA capping agent amount. Figure (3.8) Photoluminescence (PL) spectra of CdSe/CdS core/shell QDs. Figure (3.9) Electron diffraction spectroscopy (EDS) of CdSe/CdS core/shell QDs prepared via hydrothermal method. Figure (3.10) FT-IR spectrum of CdSe/CdS core/shell QDs prepared via hydrothermal method.	Figure (3.4) The color of CdSe/CdS core/shell QDs. Figure (3.5) Relation between of CdSe/CdS core/shell QDs size and TGA capping agent amount. Figure (3.6) Bandgap of CdSe/CdS core/shell QDs. Figure (3.7) Relation between CdSe/CdS core/shell QDs bandgap and TGA capping agent amount. Figure (3.8) Photoluminescence (PL) spectra of CdSe/CdS core/shell QDs. Figure (3.9) Electron diffraction spectroscopy (EDS) of CdSe/CdS core/shell QDs prepared via hydrothermal method. Figure (3.10) FT-IR spectrum of CdSe/CdS core/shell QDs prepared via hydrothermal method. Figure (3.11) XRD θ-2θ pattern of CdSe/CdS core/shell nanocrystals.	Figure (2.2)	
Figure (3.5) Relation between of CdSe/CdS core/shell QDs size and TGA capping agent amount. Figure (3.6) Bandgap of CdSe/CdS core/shell QDs. Figure (3.7) Relation between CdSe/CdS core/shell QDs bandgap and TGA capping agent amount. Figure (3.8) Photoluminescence (PL) spectra of CdSe/CdS core/shell QDs. Figure (3.9) Electron diffraction spectroscopy (EDS) of CdSe/CdS core/shell QDs prepared via hydrothermal method. Figure (3.10) FT-IR spectrum of CdSe/CdS core/shell QDs prepared via hydrothermal method.	Figure (3.5) Relation between of CdSe/CdS core/shell QDs size and TGA capping agent amount. Figure (3.6) Bandgap of CdSe/CdS core/shell QDs. Figure (3.7) Relation between CdSe/CdS core/shell QDs bandgap and TGA capping agent amount. Figure (3.8) Photoluminescence (PL) spectra of CdSe/CdS core/shell QDs. Figure (3.9) Electron diffraction spectroscopy (EDS) of CdSe/CdS core/shell QDs prepared via hydrothermal method. Figure (3.10) FT-IR spectrum of CdSe/CdS core/shell QDs prepared via hydrothermal method. Figure (3.11) XRD θ-2θ pattern of CdSe/CdS core/shell nanocrystals.	rigule (3.3)	OV-VIS SPECIFA OF CUSE/CUS COTE/SHEIF QDS.
amount. Figure (3.6) Bandgap of CdSe/CdS core/shell QDs. Figure (3.7) Relation between CdSe/CdS core/shell QDs bandgap and TGA capping agent amount. Figure (3.8) Photoluminescence (PL) spectra of CdSe/CdS core/shell QDs. Figure (3.9) Electron diffraction spectroscopy (EDS) of CdSe/CdS core/shell QDs prepared via hydrothermal method. Figure (3.10) FT-IR spectrum of CdSe/CdS core/shell QDs prepared via hydrothermal method.	amount. Figure (3.6) Bandgap of CdSe/CdS core/shell QDs. Figure (3.7) Relation between CdSe/CdS core/shell QDs bandgap and TGA capping agent amount. Figure (3.8) Photoluminescence (PL) spectra of CdSe/CdS core/shell QDs. Figure (3.9) Electron diffraction spectroscopy (EDS) of CdSe/CdS core/shell QDs prepared via hydrothermal method. Figure (3.10) FT-IR spectrum of CdSe/CdS core/shell QDs prepared via hydrothermal method. Figure (3.11) XRD θ-2θ pattern of CdSe/CdS core/shell nanocrystals.	Figure (3.4)	The color of CdSe/CdS core/shell QDs.
Figure (3.7) Relation between CdSe/CdS core/shell QDs bandgap and TGA capping agent amount. Figure (3.8) Photoluminescence (PL) spectra of CdSe/CdS core/shell QDs. Figure (3.9) Electron diffraction spectroscopy (EDS) of CdSe/CdS core/shell QDs prepared via hydrothermal method. Figure (3.10) FT-IR spectrum of CdSe/CdS core/shell QDs prepared via hydrothermal method.	Figure (3.7) Relation between CdSe/CdS core/shell QDs bandgap and TGA capping agent amount. Figure (3.8) Photoluminescence (PL) spectra of CdSe/CdS core/shell QDs. Figure (3.9) Electron diffraction spectroscopy (EDS) of CdSe/CdS core/shell QDs prepared via hydrothermal method. Figure (3.10) FT-IR spectrum of CdSe/CdS core/shell QDs prepared via hydrothermal method. Figure (3.11) XRD θ-2θ pattern of CdSe/CdS core/shell nanocrystals.	Figure (3.5)	
amount. Figure (3.8) Photoluminescence (PL) spectra of CdSe/CdS core/shell QDs. Figure (3.9) Electron diffraction spectroscopy (EDS) of CdSe/CdS core/shell QDs prepared via hydrothermal method. Figure (3.10) FT-IR spectrum of CdSe/CdS core/shell QDs prepared via hydrothermal method.	amount. Figure (3.8) Photoluminescence (PL) spectra of CdSe/CdS core/shell QDs. Figure (3.9) Electron diffraction spectroscopy (EDS) of CdSe/CdS core/shell QDs prepared via hydrothermal method. Figure (3.10) FT-IR spectrum of CdSe/CdS core/shell QDs prepared via hydrothermal method. Figure (3.11) XRD θ–2θ pattern of CdSe/CdS core/shell nanocrystals.	Figure (3.6)	Bandgap of CdSe/CdS core/shell QDs.
Figure (3.9) Electron diffraction spectroscopy (EDS) of CdSe/CdS core/shell QDs prepared via hydrothermal method. Figure (3.10) FT-IR spectrum of CdSe/CdS core/shell QDs prepared via hydrothermal method.	Figure (3.9) Electron diffraction spectroscopy (EDS) of CdSe/CdS core/shell QDs prepared via hydrothermal method. Figure (3.10) FT-IR spectrum of CdSe/CdS core/shell QDs prepared via hydrothermal method. Figure (3.11) XRD θ-2θ pattern of CdSe/CdS core/shell nanocrystals.	Figure (3.7)	
via hydrothermal method. Figure (3.10) FT-IR spectrum of CdSe/CdS core/shell QDs prepared via hydrothermal method.	via hydrothermal method. Figure (3.10) FT-IR spectrum of CdSe/CdS core/shell QDs prepared via hydrothermal method. Figure (3.11) XRD θ–2θ pattern of CdSe/CdS core/shell nanocrystals.	Figure (3.8)	Photoluminescence (PL) spectra of CdSe/CdS core/shell QDs.
	Figure (3.11) XRD θ–2θ pattern of CdSe/CdS core/shell nanocrystals.	Figure (3.9)	
Figure (3.11) XRD θ–2θ pattern of CdSe/CdS core/shell nanocrystals.		Figure (3.10)	FT-IR spectrum of CdSe/CdS core/shell QDs prepared via hydrothermal method.
	Figure (3.12) HRTEM image of CdSe/CdS core/shell QDs obtained via hydrothermal method.	Figure (3.11)	XRD θ-2θ pattern of CdSe/CdS core/shell nanocrystals.
Figure (3.12) HRTEM image of CdSe/CdS core/shell QDs obtained via hydrothermal method.		Figure (3.12)	HRTEM image of CdSe/CdS core/shell QDs obtained via hydrothermal method.

Figure (3.13)	Absorption spectrum and (B) energy band-gap of the as-synthesized CdSe/CdS core/shell QDs.
Figure (3.14)	Energy Dispersive Spectroscopy (EDS) of CdTe/CdS core/shell QDs obtained via hydrothermal method.
Figure (3.15)	X-Ray Diffraction (XRD) of CdTe/CdS core/shell QDs obtained via hydrothermal method at 120 °C (A) and 170 °C (B).
Figure (3.16)	FT-IR spectrum of CdTe/CdS core/shell QDs obtained via hydrothermal method.
Figure (3.17)	HRTEM image of CdTe/CdS core/shell QDs obtained via hydrothermal method.
Figure (3.18)	(A) Absorption spectrum and (B) energy band-gap of the as-synthesized CdTe/CdS core/shell QDs at 170 °C.
Figure (3.19)	Energy Dispersive Spectroscopy (EDS) of CdZnSe/CdS and CdZnSe/ZnS core/shell QDs obtained via hydrothermal method.
Figure (3.20)	X-Ray Diffraction (XRD) of CdZnSe/CdS and CdZnSe/ZnS core/shell QDs obtained via hydrothermal method.
Figure (3.21)	FT-IR spectrum of CdZnSe/CdS and CdZnSe/ZnS core/shell QDs obtained via hydrothermal method.
Figure (3.22)	HRTEM image of CdZnSe/CdS and CdZnSe/ZnS core/shell QDs obtained via hydrothermal method.
Figure (3.23)	(A) Absorption spectrum and (B) energy band-gap of the as-synthesized CdZnSe/CdS and CdZnSe/ZnS core/shell QDs at 170 °C.
Figure (3.24)	Energy Dispersive Spectroscopy (EDS) of CdZnTe/CdS and CdZnTe/ZnS (core/shell) QDs obtained via hydrothermal method.
Figure (3.25)	X-Ray Diffraction (XRD) of CdZnTe/CdS and CdZnTe/ZnS (core/shell) QDs obtained via hydrothermal method.
Figure (3.26)	FT-IR spectrum of CdZnTe/CdS and CdZnTe/ZnS (core/shell) QDs obtained via hydrothermal method.

Figure (3.27)	HRTEM image of CdZnTe/CdS and CdZnTe/ZnS (core/shell) QDs obtained via hydrothermal method.
Figure (3.28)	(A) Absorption spectrum and (B) energy band-gap of the as-synthesized CdZnTe/CdS and CdZnTe/ZnS (core/shell) QDs at 170 °C.
Figure (3.29)	Energy Dispersive Spectroscopy (EDS) of CdSeTe/CdS core/shell QDs obtained via hydrothermal method.
Figure (3.30)	X-Ray Diffraction (XRD) of CdSeTe/CdS core/shell QDs obtained via hydrothermal method.
Figure (3.31)	FT-IR spectrum of CdSeTe/CdS core/shell QDs obtained via hydrothermal method.
Figure (3.32)	HRTEM image of CdSeTe/CdS core/shell QDs obtained via hydrothermal method.
Figure (3.33)	(A) Absorption spectrum and (B) energy band-gap of the as-synthesized CdSeTe/CdS core/shell QDs at 170 °C.
Figure (3.34)	Energy Dispersive Spectroscopy (EDS) of CdZnSeTe/CdS and CdZnSeTe/ZnS core/shell QDs obtained via hydrothermal method.
Figure (3.35)	X-Ray Diffraction (XRD) of CdZnSeTe/CdS and CdZnSeTe/ZnS core/shell QDs obtained via hydrothermal method.
Figure (3.36)	FT-IR spectrum of CdZnSeTe/CdS and CdZnSeTe/ZnS core/shell QDs obtained via hydrothermal method.
Figure (3.37)	HRTEM image of CdZnSeTe/CdS and CdZnSeTe/ZnS core/shell QDs obtained via hydrothermal method.
Figure (3.38)	(A) Absorption spectrum and (B) energy band-gap of the as-synthesized CdZnSeTe/CdS and CdZnSeTe/ZnS core/shell QDs at 170 °C.
Figure (3.39)	High-resolution XPS analysis of the three constituent elements in CuZnS nanocrystals: copper 2p, zinc 2p, and sulfur 2 p. High-resolution XPS analysis of the three constituent elements in CuZnS nanocrystals: copper 2p, zinc 2p, and sulfur 2 p.